A Novel Calcium-Independent Peripheral Membrane-Bound Form of Annexin B12[†]

Balachandra G. Hegde,[‡] J. Mario Isas,[‡] Guido Zampighi,[§] Harry T. Haigler,*[,||] and Ralf Langen*[,‡]

Department of Biochemistry and Molecular Biology, Zilkha Neurogenetic Institute, University of Southern California, Keck School of Medicine, Los Angeles, California 90033, Department of Neurobiology and Jules Stein Eye Institute, University of California—Los Angeles, School of Medicine, Los Angeles, California 90095, and Department of Physiology and Biophysics, University of California—Irvine, Irvine, California 92697

Received October 20, 2005; Revised Manuscript Received November 20, 2005

ABSTRACT: Annexins are soluble proteins that can interact with membranes in a Ca^{2+}-dependent manner. Recent studies have shown that they can also undergo Ca^{2+}-independent membrane interactions that are modulated by pH and phospholipid composition. Here, we investigated the structural changes that occurred during Ca^{2+}-independent interaction of annexin B12 with phospholipid vesicles as a function of pH. Electron paramagnetic resonance analysis of a helical hairpin encompassing the D and E helices in the second repeat of the protein showed that this region refolded and formed a continuous amphipathic α helix following Ca^{2+}-independent binding to membranes at mildly acidic pH. At pH 4.0, this helix assumed a transmembrane topography, but at pH ∼5.0−5.5, it was peripheral and approximately parallel to the membrane. The peripheral form was reversibly converted into the transmembrane form by lowering the pH and vice versa. Furthermore, analysis of vesicles incubated with annexin B12 using freeze-fracture electron microscopy methods showed classical intramembrane particles at pH 4.0 but none at pH 5.3. Together, these data raise the possibility that the peripheral-bound form of annexin B12 could act as a kinetic intermediate in the formation of the transmembrane form of the protein.

Annexins represent a highly conserved family of membrane-binding proteins that are typically expressed in high levels in nearly all cell types of multicellular organisms (*1*−*3*). Annexins have been implicated in a number of membrane-related events, but their exact physiological roles are only partially understood (*1*, *3*). A hallmark of annexins is their ability to reversibly interact with negatively charged lipids in the presence of Ca^{2+} (*4*). Several lines of evidence showed that this Ca^{2+}-bound form was structurally related to the soluble, lipid-free form for which high-resolution crystal structures exist (*4*−*8*). As illustrated with the example of the crystal structure of annexin B12 (*9*), annexins are typically made of four highly homologous and structurally conserved repeat regions (Figure 1). Each of these repeat regions contains four helical bundles (helices A, B, D, and E), with helix C running approximately perpendicular to the helical bundle. The convex side of the molecule contains four A−B and four D−E interhelical loop regions, which mediate Ca^{2+}-dependent binding to the surface of membranes. This membrane interaction is thought to occur by a Ca^{2+}-bridging mechanism, in which the A−B and D−E loop regions and negatively charged phospholipid headgroups on the surface of bilayers jointly coordinate Ca^{2+} (*10*).

In addition to this Ca^{2+}-dependent membrane-bound form, significant recent evidence demonstrated that a number of annexins can also interact with cellular and phospholipid membranes in the absence of Ca^{2+} (*11*−*18*). At least in the examples investigated to date, the Ca^{2+}-independent interaction of annexins with membranes is dependent upon the pH and lipid composition. For instance, our studies of annexin B12 showed that the pH-dependent membrane interaction occurred with half-maximal binding at pH ∼5.8 for phosphatidylserine-containing vesicles and at pH ∼6.5 for cardiolipin-containing vesicles (*12*).

The most extensive structural studies of Ca^{2+}-independent membrane association of annexins used the reversible interaction of annexin B12 with large phosphatidylserine-containing vesicles at pH 4.0 as a model system (*12*, *13*, *16*, *19*). When bound to vesicles at pH 4.0, large-scale changes in the tertiary structure were observed that dramatically changed the structure in all four repeats (*12*). The protein did not simply unfold, as evidenced by the fact that it retained the predominantly α-helical secondary structure observed in the crystal structure (*12*). Electron paramagnetic studies of the helical hairpin regions that encompass an A−B helix (*13*) and a D−E helix (*16*) in the crystal structure showed that these regions refolded and formed continuous transmembrane helices in the membrane-bound state at pH 4.0 (see Figure 1B). These transmembrane helices were amphipathic, with one face exposed to the hydrophobic core of the lipid bilayer and one face exposed to an aqueous pore (*13*, *16*) that mediated channel-like activity (*19*). The hydrophobic faces of the transmembrane helices were formed by mainly hydrophobic amino acid side chains that were buried in the core of the crystal structure (*13*, *16*). However, the hydro-

[†] This work was supported by National Institutes of Health Grants GM 63915 (to R.L.), GM 55651 (to H.T.H.), and EY-04110 (to G.Z.).

* To whom correspondence should be addressed. Telephone: 323-442-1323. Fax: 323-442-4404. E-mail: langen@usc.edu (R.L.); Telephone: 949-824-6304. Fax: 949-824-8540. E-mail: hhaigler@uci.edu (H.T.H.).

[‡] University of Southern California.

[§] University of California—Los Angeles.

[||] University of California—Irvine.

10.1021/bi052143+ CCC: $33.50
Published on Web 12/24/2005

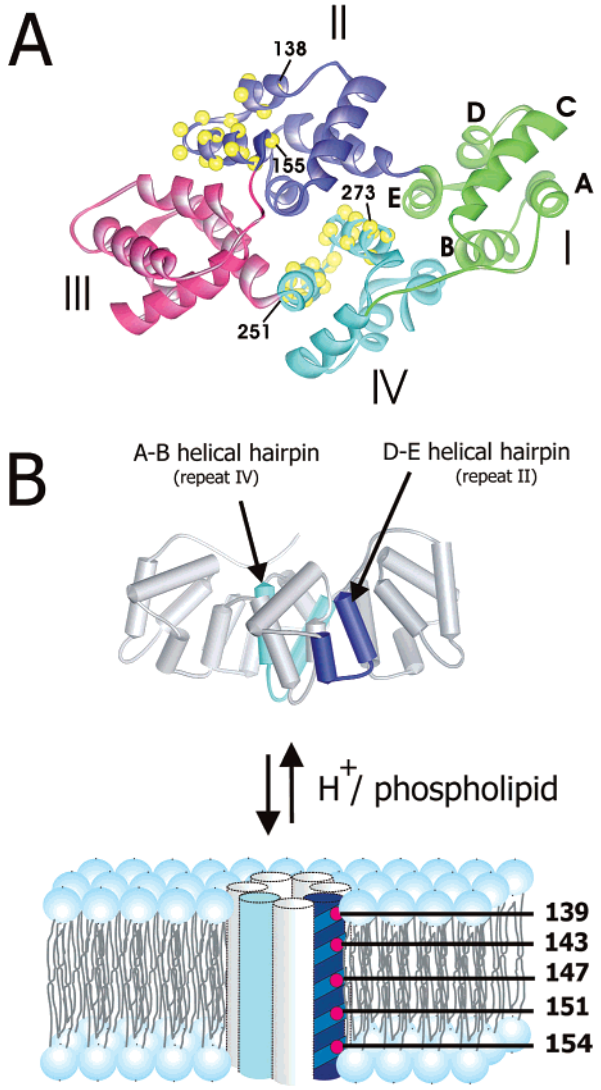

FIGURE 1: Structure of annexin B12 and pH-dependent transmembrane insertion. (A) Crystal structure of an annexin 12 monomer (*9*) (PDB 1AEI). Each of the four repeats (shown in different colors) in the core domain contains five helices (A−E). The two helical hairpin regions that have been studied by nitroxide-scanning experiments are highlighted with yellow spheres on the α carbons. (B) Hypothetical model of the transmembrane form of annexin B12 at pH 4.0. The two helical hairpin regions highlighted by α-carbon spheres in A undergo inside-out refolding when exposed to membranes at pH 4.0 and form the two transmembrane amphipathic helices highlighted in blue and light green in B. The locations of the lipid-exposed residues in the transmembrane helix formed by the D−E helical hairpin are noted. This region was the focus of studies reported herein.

phobic face of these otherwise typical amphipathic helices also contained some acidic residues. Protonation of these carboxylate residues on or near the hydrophobic faces of the transmembrane helices was proposed to trigger H^+-induced membrane association (*13*, *16*). Inspection of the amino acid sequence of annexin B12 reveals seven helical hairpins that could potentially refold into amphipathic transmembrane helices following protonation of carboxylate-switch residues (*13*, *16*). Fluorescence spectroscopy experiments confirmed the transmembrane nature of the D−E helical region (*20*) and showed that the transmembrane form of annexin B12 was mainly monomeric (*21*). On the basis of these studies, we speculated that the channel-like activity of annexin B12 at mildly acidic pH is mediated by a pore formed by perhaps

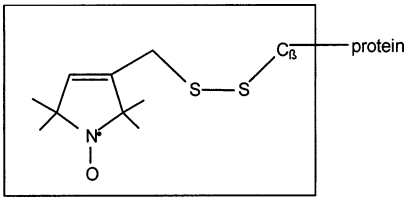

FIGURE 2: Structure of the R1 side chain.

as many as seven transmembrane helices from the same protein molecule (see the model in Figure 1B); however, several aspects of this model have not yet been tested.

The detailed molecular mechanism that allows soluble annexin B12 to reversibly transition into a transmembrane protein remains an open question. Studies on other membrane-inserting proteins have shown that the formation of a transmembrane structure might be a stepwise mechanism that proceeds via the formation of a membrane surface-bound intermediate structure (*22*). Although most of the previous structural studies of the Ca^{2+}-independent binding of annexin B12 to membranes have been performed at pH 4.0, limited studies at intermediate pH values raise the possibility that these conditions may provide a useful window for studying intermediates in the annexin B12 insertion pathway. One study showed that there was global refolding at all pH values, which supported Ca^{2+}-independent membrane binding of annexin B12, but these studies did not evaluate the topography of the protein (*12*). The possibility that several types of topographies could exist for different Ca^{2+}-independent membrane interactions was suggested by another study that employed a commonly used lipophilic probe to test for annexin B12 membrane insertion (*19*). While labeling was observed at pH 4−5, significantly less labeling and presumably less membrane insertion were observed at pH 5.6. In the present study, we addressed the mechanism of Ca^{2+}-independent membrane insertion of annexin B12 by examining the structure of the membrane-bound protein at various acidic pH values using site-directed spin labeling (SDSL)[1] and freeze-fracture electron microscopy.

SDSL involves the covalent addition of a paramagnetic nitroxide side chain such as R1 (Figure 2) to specific cysteine residues that are engineered into selected sites in the protein after endogenous cysteine residues are replaced (*23*). The electron paramagnetic resonance (EPR) spectrum of R1 on the protein is sensitive to the environment of the nitroxide and can be used to evaluate local structure and conformational changes (*24*). EPR accessibility parameters provide a sensitive and reliable method for determining the depth of insertion of R1 into membranes (*25*). This method is based on the differential accessibility of lipid-exposed R1 side chains to colliders of different polarity such as O_2 or NiEDDA. While the more hydrophobic O_2 preferentially partitions into the membrane, the more hydrophilic NiEDDA is preferentially excluded from the hydrophobic core of the membrane. Systematic studies have shown that the ratio of

[1] Abbreviations: EPR, electron paramagnetic resonance; PS, phosphatidylserine from a biological source; POPS, 1-palmitoyl-2-oleoyl-*sn*-glycero-3-[phospho-L-serine]; PC, phosphatidylcholine from a biological source; POPC, 1-palmitoyl-2-oleoyl-*sn*-glycero-3-phosphocholine; R1, the nitroxide side chain illustrated in Figure 2; SDSL, site-directed spin labeling; $\Pi(O_2)$, accessibility of the R1 side chain to O_2; Π(NiEDDA), accessibility of the R1 side chain to NiEDDA.

the respective accessibilities is a direct measure of the immersion depth of the R1 side chain *(23, 25)*. Nitroxide scans in which single native side chains are sequentially replaced with R1 can be analyzed for the depth of insertion and thereby provide a powerful method for determining the topography of membrane proteins (*25*).

In the current study, we analyzed a nitroxide scan from residues 139 to 155 located in a D−E helical hairpin region of annexin B12 (see Figure 1B) at pH values that support Ca^{2+}-independent binding of annexin B12 to large phosphatidylserine-containing vesicles. The data show that a previously described transmembrane helix structure formed by this region at pH 4.0 (*16*) is converted to a peripherally bound α helix at pH values in the range of 5.0−5.5. To obtain more global structural information regarding the structure of the transmembrane form of the protein, we used freeze-fracture electron microscopy to study annexin B12 bound to phospholipid vesicles in the absence of Ca^{2+}. Intramembrane particles were observed at pH 4.0 but not at pH 5.3. When these experiments are taken together, they provide additional characterization of the transmembrane form of annexin B12 and identified a novel interfacial form that may be a kinetic intermediate in the insertion pathway.

EXPERIMENTAL PROCEDURES

Protein Expression and Purification. Recombinant annexin B12 with single-cysteine mutations successively at positions 139−155 were expressed in DH5α *Escherichia coli* cells and purified by reversible Ca^{2+}-dependent binding to phospholipid vesicles followed by column chromatography, as described previously (*12*, *16*). The purified proteins were stored at −80 °C in 20 mM HEPES buffer at pH 7.4, containing 100 mM NaCl (HEPES-NaCl) in the presence of 1 mM dithiothreitol (DTT).

Spin Labeling. Prior to spin labeling, DTT was removed with PD-10 columns (Amersham Biosciences) that were equilibrated with HEPES-NaCl buffer. Spin label (1-oxyl-2,2,5,5-tetramethyl-Δ3-pyrroline-3-methyl) methanethiosulfonate, MTSL (Toronto Research Chemicals, Canada), in 4× molar excess, was added to the protein in HEPES-NaCl buffer and incubated overnight at 4 °C. The unreacted spin label was removed with PD-10 columns that were equilibrated with HEPES-NaCl buffer. Spin-labeled protein was stored at 4 °C. Spin-labeled mutants of annexin B12 are designated by giving the sequence position of the cysteine substitution followed by the code of the nitroxide spin label, R1.

Vesicle Preparation and Copelleting Assay. Large vesicles were prepared according to the method of Reeves and Dowben (*26*) using a 2:1 (w/w) ratio of phosphatidylserine and phosphatidylcholine from Avanti Polar Lipids (Alabaster, AL). The phospholipids were from either a biological source (PS, brain, catalog number 840032C; PC, egg yolk, catalog number 840051) or chemically synthesized (POPS, 1-palmitoyl-2-oleoyl-*sn*-glycero-3-[phospho-L-serine], catalog number 840034C; POPC, 1-palmitoyl-2-oleoyl-*sn*-glycero-3-phosphocholine, catalog number 850457). Vesicles containing PS/PC were used for the freeze-fracture experiments. Most EPR experiments were performed with vesicles containing both PS/PC and POPS/POPC, but all of the reported studies used vesicles containing POPS/POPC. Both types of lipid gave nearly identical results for binding and EPR mobility studies, but vesicles containing POPS/POPC had less batch/batch variability in EPR accessibility parameters.

In the vesicle copelleting assays, 10 μg of spin-labeled or cysteine-free annexin B12 was mixed with 200 μg of phospholipid POPS/POPC vesicles at the appropriate pH (100 mM sodium acetate buffer for a pH range of 4−5.5, 100 mM MES buffer for a pH range of 6−6.5, and 20 mM HEPES and 100 mM NaCl buffer for a pH range of 7−7.4) and incubated at room temperature for about 15−30 min before centrifugation to pellet the vesicles along with the associated protein. Aliquots of the supernatant (concentrated down to 20 μL) were analyzed by polyacrylamide gel electrophoresis, followed by Coomassie blue staining.

EPR Measurements. For EPR experiments, ∼30 μg of spin-labeled protein was mixed with 600 μg of POPS/POPC vesicles at the appropriate pH values (100 mM sodium acetate buffer for a pH range of 4−5.5) and incubated for about 15−30 min before centrifugation at 4 °C. The protein/phospholipid molar ratio was ∼1:1000. The pellet was suspended in a small volume of the appropriate pH buffer and loaded into TPX capillaries. EPR spectra were recorded at room temperature with a Bruker EMX X-band EPR spectrometer fitted with either a Bruker ER4123D dielectric resonator or an ER4119HS resonator. In the indicated cases, we recorded EPR spectra of concentrated samples of R1-labeled annexin B12 in solution in either the presence or absence of 30% sucrose to reduce protein tumbling. All spectra are shown with a magnetic field scan width of 100 G.

The EPR power saturation method was used to measure the oxygen and NiEDDA accessibility (*23*, *25*). The oxygen concentration was that of oxygen in equilibrium with air, and the NiEDDA concentration was 100 mM. The membrane immersion depth, *d*, for R1-labeled residues was calculated from the parameter $\Phi = \ln \Pi(O_2)/\Pi(\text{NiEDDA})$ (*23*, *25*). The calibration of Φ in terms of depth at various pH values was obtained with the use of 1-palmitoyl-2-stearoyl-(DOXYL)-*sn*-glycero-3-phosphocholine, with the spin label attached at the 7, 10, and 12 positions on the acyl chains, as described (*25*). The following equations were used to calculate the depth at pH values: $d[\text{Å}] = 5.0\Phi + 8.7$ at pH 4, $d[\text{Å}] = 5.7\Phi + 6.6$ at pH 4.5, $d[\text{Å}] = 7.0\Phi + 2.8$ at pH 5, and $d[\text{Å}] = 7.40\Phi - 3.1$ at pH 5.5.

Freeze-Fracture Electron Microscopy. For freeze-fracture analysis, annexin B12 (13 μg) was incubated at room temperature with PS/PC vesicles (780 μg). For cryoprotection, 10% glycerol was added. Aliquots (∼0.5 μL) were deposited on a gold-coated specimen holder and frozen rapidly by immersion in liquid propane. The frozen specimen was then transferred to a Balzer 100K freeze-fracture apparatus and fractured at −120 °C and 10^{-7} mbar. The fractured surface was then coated with platinum at 80 °C and with carbon at 90 °C. Specimens were coated with 0.5% colloidon in amyl acetate to avoid fragmentation of the replica and cleaned with bleach. Replicas were washed in distilled water and deposited on Formvar-coated single-hole copper grids. Colloidon was removed by immersion in amyl acetate, and replicas were observed in a Zeiss 10C electron microscope. Particle dimensions were determined by measuring distances perpendicular to the direction of the shadowing.

Each particle appears as a dark zone, and the cone extending from it was used to define the direction of the shadowing.

RESULTS

Analysis of Ca^{2+}-Independent Membrane Association of Annexin B12 as a Function of pH. Our previous studies demonstrated that annexin B12 can associate with membranes in a Ca^{2+}-independent mechanism at mildly acidic pH (*12*, *13*, *16*, *19*). The protein underwent global changes in the tertiary structure at all pH values that induced membrane association (*12*), and detailed studies showed that transmembrane helices formed at pH 4.0 (*6*, *13*). Chemical-labeling experiments with a lipophilic probe were consistent with the transmembrane form under those conditions (*19*). However, at intermediate pH values, the labeling data suggested the existence of a Ca^{2+}-independent membrane-associated form that did not appear to be strongly exposed to the hydrophobic interior of the bilayer (*19*). The following experiments were designed to investigate this potentially new structural form of annexin B12.

First, a copelleting assay was performed to define the Ca^{2+}-independent membrane-binding properties of the protein under the exact conditions that were to be used in subsequent EPR experiments. Annexin B12 was incubated with large phospholipid vesicles [2:1 (w/w) POPS/POPC], after which the mixture was centrifuged to pellet the vesicles along with any associated protein. Aliquots of the supernatant were analyzed by gel electrophoresis followed by Coomassie blue staining and showed that annexin B12 quantitatively copelleted with the vesicles if the pH value was between pH 4.0 and 5.3, but no vesicle association was detected at neutral pH (Figure 3A). Minor amounts of unbound protein were detected at pH 5.5. Ca^{2+}-Dependent membrane interaction of annexin B12 is highly cooperative, requiring ~20 μM free Ca^{2+} (*27*), a concentration that is several orders of magnitude greater than any residual Ca^{2+} present in the buffers used in the current study. Thus, the pH-dependent membrane interaction observed here is clearly Ca^{2+}-independent. This notion is supported by previous observations that the presence of EGTA in the buffer did not affect the pH-dependent membrane interaction of annexin B12 (*12*, *19*).

Our previous SDSL studies (*16*) showed that residues 138−158 of annexin B12 were a helical hairpin in solution but were converted to a continuous transmembrane helix upon membrane association at pH 4.0 (Figure 1B). The residues in this scan that were the most deeply imbedded in the membrane at pH 4.0 (*16*), 147R1 and 151R1, were used as reporters to extend our EPR studies of this region to intermediate pH values. As previously shown (*16*), in the absence of membranes, the spectra for 147R1 and 151R1 were similar in solution at pH 7.4 and at 4.0 (red spectra in Figure 3B). Figure 3B also shows that incubation at intermediate pH values in the absence of membranes did not induce any spectral changes in these sites. However, the spectra of 147R1 and 151R1 underwent significant changes under all conditions where Ca^{2+}-independent membrane association occurred (black spectra in Figure 3B). The spectral changes indicate that these two sites, which were highly constrained because of their position in the core of the soluble protein, became moderately mobile in the membrane-bound state. The spectra of both sites in the Ca^{2+}-independent membrane-bound state were similar at all pH values tested (Figure 3B).

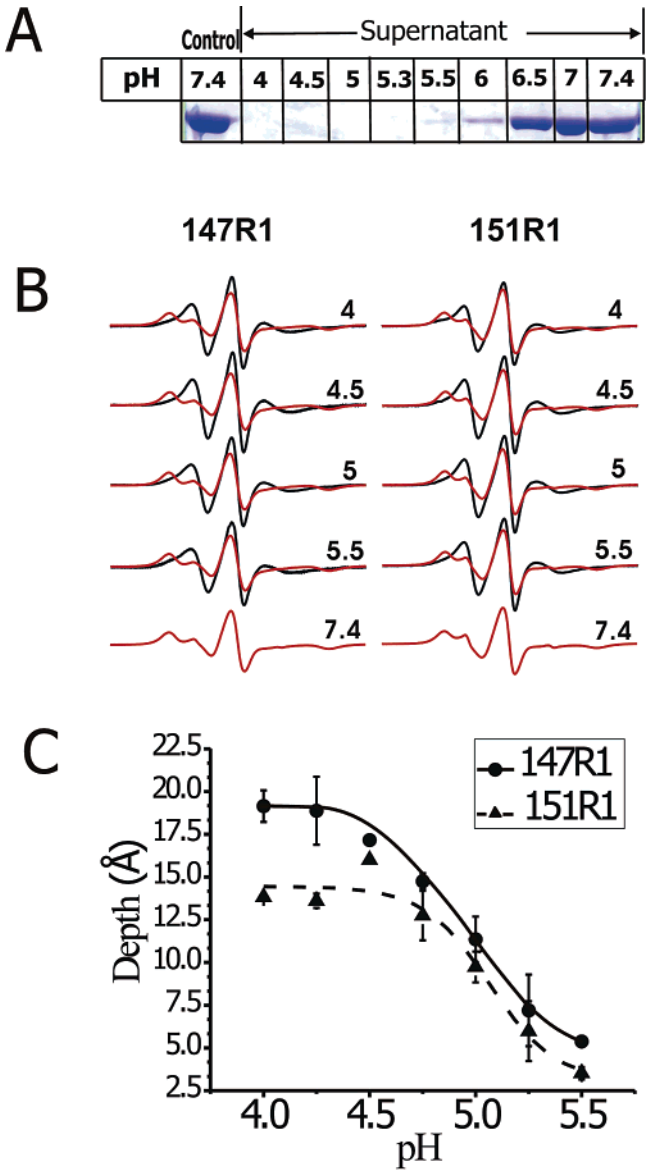

FIGURE 3: pH dependence of Ca^{2+}-independent annexin B12 binding. (A) Annexin B12 was incubated at room temperature with large phosphatidylserine-containing vesicles at the indicated pH and then centrifuged to pellet the vesicles along with the associated protein. The conditions were identical to those used for the EPR experiments (see the Experimental Procedures). Aliquots of the supernatant were analyzed by polyacrylamide gel electrophoresis followed by Coomassie blue staining, and the region of the gel that contained the annexin B12 band is shown. The lack of Coomassie blue staining material in this area indicates complete association of the protein with vesicles. The "control" band is from a sample that contained annexin B12 but no vesicles. (B) EPR spectra of 147R1 and 151R1 in solution (red traces) and bound to vesicles (black traces) at the indicated pH. Because the protein did not associate with vesicles at pH 7.4 in the absence of Ca^{2+}, only the spectra for the soluble protein are shown. (C) Depth of membrane insertion of 147R1 (●, —) and 151R1 (▲, - - -) in vesicles at the indicated pH values was determined by methods described in the Experimental Procedures. Each data point is the mean of four independent experiments that involved at least two separate preparations of protein and vesicles.

The following experiments determined the depth of membrane insertion of 147R1 and 151R1 as a function of

pH by measuring the EPR accessibility parameters $\Pi(O_2)$ and Π(NiEDDA). Because O_2 and NiEDDA are preferentially included and excluded, respectively, in the hydrophobic region of bilayers, the ratio of $\Pi(O_2)$ and Π(NiEDDA) can be used to determine the immersion depth (see the Experimental Procedures). As expected from previous studies (*16*), the immersion depths for 147R1 and 151R1 were ~18 and ~13 Å, respectively, at pH 4.0 (Figure 3C). Little change was noted at pH 4.5, but at higher pH values, the immersion depth of 147R1 and 151R1 decreased systematically to values of ~4−6 Å, respectively, at pH 5.5 (Figure 3C). Thus, the transmembrane structure present below pH 4.5 was disrupted at higher pH values.

Analysis of the 139−155 Nitroxide Scan of Annexin B12. Experiments presented in Figure 3 showed that annexin B12 bound quantitatively to membranes in a Ca^{2+}-independent manner in the pH range of 4.0−5.3. The structure of the membrane-bound protein at the higher end of this pH range, however, must be different from the transmembrane form that previously had been characterized at pH 4.0 (*13*, *16*). To further investigate the nature of these structural differences, a nitroxide-scanning experiment was performed in which each side chain from position 139 to 155 was replaced with the R1 spin label. Nitroxide-labeled derivatives were investigated by EPR spectroscopy at pH 5.3 in the presence or absence of vesicles. Because the protein binds quantitatively to vesicles at pH 5.3, there was no signal from unbound protein in EPR spectra recorded in the presence of vesicles (Figure 3A). The absence of soluble protein was further verified by cosedimenation experiments in which R1-labeled annexin B12 derivatives were pelleted together with the vesicles at pH 5.3. No signal from soluble protein could be detected in the supernatant (data not shown). Sucrose (30%) was included in the buffer of samples analyzed in the absence of vesicles to reduce the tumbling of the soluble protein. Because the tumbling of both the soluble protein in the presence of 30% sucrose and membrane-bound protein was slow on the EPR time scale, the EPR spectra of both states mainly reflected the local motion of the spin label.

In general, the spectra for soluble annexin B12 at pH 5.3 in the absence of membranes (red traces in Figure 4) are nearly identical to those described earlier for soluble annexin B12 at neutral pH (*28*), thereby indicating that the structure of the soluble protein at pH 5.3 was similar to that of the crystal structure of the protein. Because the excellent agreement between the EPR spectra at neutral pH and the crystal structure was discussed in detail previously (*28*), only a few selected examples are noted here to re-illustrate this point. Residues 144 and 145 are located in loops in the crystal structure and display a very high degree of mobility, as evidenced by the sharp and narrowly spaced EPR spectra lines (red traces in Figure 4). In contrast, the spectra of positions that are buried in the core of the crystal structure of the protein (e.g., residues 139, 147, 151, and 154) indicate highly constrained mobility (see the arrows highlighting the highly immobilized spectral components in the red traces in Figure 4).

Upon membrane binding at pH 5.3, however, major EPR spectral changes can be observed at nearly every site. For example, the EPR spectra of the loop sites 144R1 and 145R1 no longer indicate a high degree of motion; rather, the spectra from these sites indicated the formation of an ordered

FIGURE 4: EPR spectra of the 139−155 nitroxide scan of annexin B12. The EPR spectra of the indicated R1-labeled derivatives of annexin B12 were recorded in solution in the presence of 30% sucrose (red traces) or when bound to phosphatidylserine-containing vesicles at pH 5.3 in the absence of Ca^{2+} (black traces). The red arrows point to spectral features characteristic of highly immobilized nitroxide side chains.

structure (black traces in Figure 4). After membrane binding, major spectral changes are also observed at sites that are buried in the soluble protein. In these cases, membrane interaction causes an increase in the motion, as indicated by the sharper lines and the loss of the highly immobilized spectral components (e.g., see 139R1, 147R1, 151R1, and 154R1 in the black traces in Figure 4). These data clearly indicate that these sites are no longer buried in the protein after pH-induced membrane interaction. This behavior is reminiscent of the conformational changes that were observed at pH 4.0, in which buried hydrophobic residues of the solution structure became more mobile when the protein refolded and exposed the previously buried sites to the hydrophobic interior of the membrane (*13*, *16*). In fact, the spectra for membrane-bound annexin B12 derivatives at pH 5.3 are qualitatively similar to those previously obtained at pH 4 (*16*). However, these studies of mobility do not address the question of the membrane topography of the protein.

To further investigate the structure of membrane-bound annexin B12 at pH 5.3, we determined the relative O_2 and NiEDDA accessibilities of the 139−155 nitroxide scan. Both $\Pi(O_2)$ and Π(NiEDDA) exhibited periodic oscillations as a function of the amino acid sequence position in which both maxima are spaced 3−4 amino acids apart (Figure 5A). Minima also had this same spacing (Figure 5A). Such a periodicity is a characteristic feature of a helical structure, which has a periodicity of 3.6 amino acids/turn. Importantly, the periodic oscillations for $\Pi(O_2)$ and Π(NiEDDA) are 180°

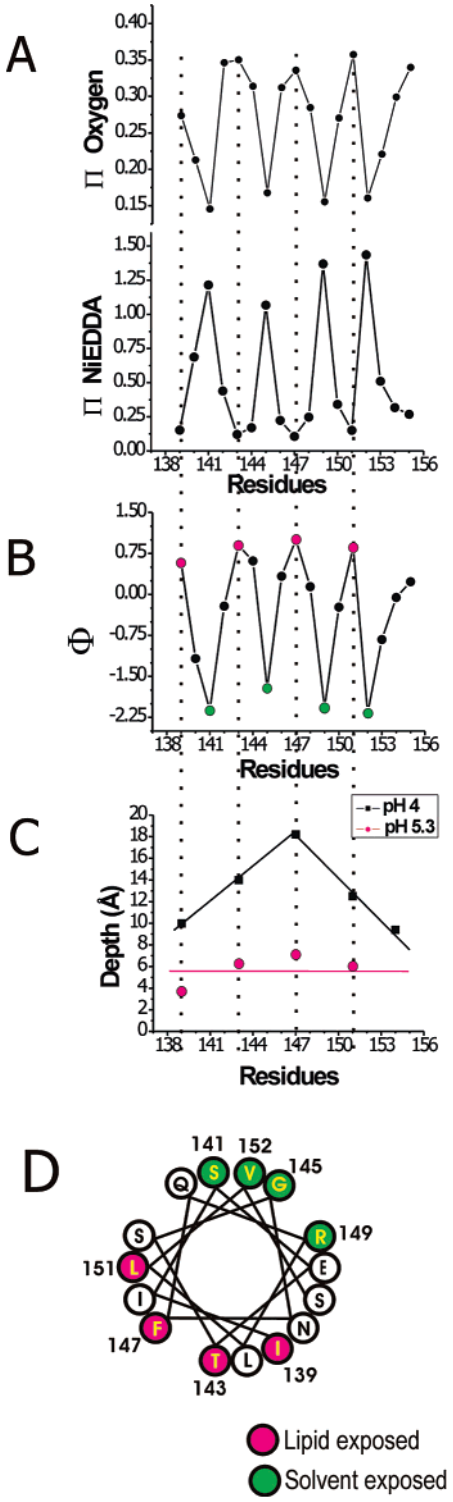

FIGURE 5: Sequence dependence of EPR accessibility parameters of annexin B12 in the membrane-bound state. (A) EPR accessibility parameters $\Pi(O_2)$ and Π(NiEDDA) were determined (see the Experimental Procedures) for the indicated R1-labeled derivatives of annexin B12 following the binding to phosphatidylserine-containing vesicles at pH 5.3 in the absence of Ca^{2+}. (B) Φ values for R1 side chains were calculated from the data in A. Local maxima and minima are highlighted with symbols that are red and green, respectively. (C) Insertion depth of residues in the scanned region that are maximally exposed to lipid was determined for R1-labeled derivatives of annexin B12 at pH 5.3 based on data presented in B (red curve) or at pH 4.0 based on previously reported studies (black curve) (*16*). (D) Helical wheel presentation of the scanned region at pH 5.3 with the individual positions color-coded on the basis of the data presented in B.

out-of-phase. Such a pattern is highly characteristic of an asymmetrically solvated helical structure that is exposed to the lipid on one face and to the aqueous environment on the other face. The $\Pi(O_2)$ and Π(NiEDDA) data can be conveniently summarized by the parameter $\Phi = \ln \Pi(O_2)/\Pi$(NiEDDA). A plot of Φ as a function of the amino acid sequence shows a clear periodicity of both maximal (red circles in Figure 5B) and minimal (green circles in Figure 5B) values corresponding to residues that are maximally exposed to the lipid and the aqueous environment, respectively. When residues with maximal (red circles) and minimal (green circles) Φ values were plotted on a helical wheel, lipid-exposed residues fell onto one face and solvent-exposed sites fell onto the opposite face (Figure 5D). In a previous study of annexin B12 at pH 4.0, 154R1 had a local peak in the Φ value and was thought to be exposed to lipid in a transmembrane helix (*16*). However, there is not an unambiguous maximal Φ value at or adjacent to position 154 for membrane-associated annexin B12 at pH 5.3 (Figure 5B). Although it is clear that membrane-bound annexin B12 at pH 5.3 contains an amphipathic helix in the 139−151 region, the data do not clearly define the secondary structure of the 152−155 region.

Regardless of the minor details of the exact extent of the length of the helix, the helical structure at pH 5.3 defined in Figure 5 has one major distinction compared with the transmembrane helix that forms at lower pH values. At pH 5.3, the Φ values of the membrane-exposed sites were very similar to each other, resulting in highly similar immersion depths of approximately 4−7 Å (red symbols in Figure 5C). These values are in striking contrast to the immersion depth previously defined for this region in the transmembrane state at pH 4.0 (reproduced from ref *16* in the black symbols in Figure 5C). At pH 4.0, most immersion depth values were much larger, and furthermore, the change in immersion depth was on the order of ∼4−5 Å/turn, as is characteristic for transmembrane helices (*16*). In contrast, the variations in the immersion depth at pH 5.3 are much smaller and no longer consistent with a transmembrane structure. Rather, the consistently shallow immersion depths are characteristic for peripherally bound helices. Taken together, the present study therefore indicates that the scanned region of annexin B12 assumes a peripherally bound helical structure at pH 5.3, rather than the transmembrane helix that was previously detected at pH 4.0 (*16*).

The data presented above show that the helix−loop−helix structure present in aqueous solution can assume two distinctively different structural states upon pH-dependent membrane interaction. While this region is predominantly in a transmembrane helix orientation at pH 4−4.5, a peripherally bound continuous helical structure forms at higher pH values. We previously demonstrated that the formation of the transmembrane form was reversible (*16*). When the transmembrane form of membrane-bound annexin B12 at pH 4.0 subsequently was exposed to neutral pH, the protein dissociated from the membrane and refolded into its soluble form (*16*). In the current study, cosedimentation experiments parallel to those shown in Figure 3A showed that the membrane-associated state generated at pH 5.3 was released from the membrane by raising the pH to 7.4 (data not shown). The interconversion of the different membrane-bound forms of annexin B12 was further investigated using

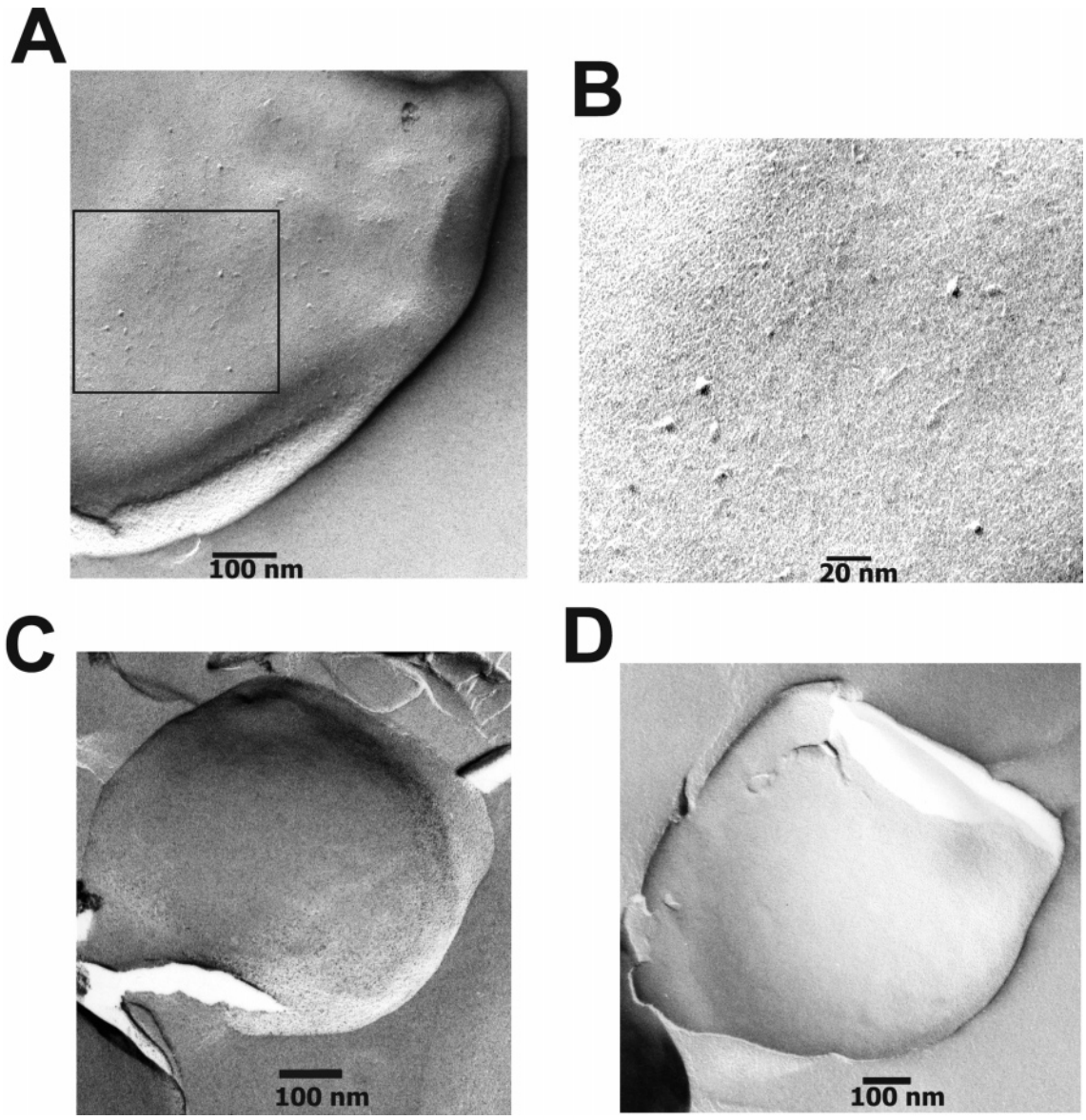

FIGURE 6: Freeze-fracture microscopy analysis of Ca^{2+}-independent membrane binding of annexin B12. Annexin B12 was bound to phosphatidylserine-containing vesicles at the indicated pH and then processed for freeze-fracture microscopy analysis as described in the Experimental Procedures. The micrographs are from vesicles incubated with annexin B12 at either pH 4.0 (A and B) or pH 5.3 (C). A micrograph of vesicles incubated in the absence of annexin B12 at pH 4.0 is shown in D.

EPR analysis of the immersion depth of 147R1 as a reporter. The peripheral form of the protein was formed by incubating 147R1 with vesicles at pH 5.3; the pH was then lowered to pH 4.5, and the immersion depth was determined to be 16.0 $\pm$ 1.1 Å. Because this value is similar to that obtained when 147R1 was directly exposed to vesicles at pH 4.5 (see Figure 3C), the experiment indicates that the surface-bound helix can transition to the transmembrane form at lower pH values. The reversibility in the opposite direction was tested by incubating 147R1 with vesicles at pH 4.5 to generate the transmembrane form and then measuring the immersion depth at pH 5.3. Under these conditions, the immersion depth was 8.1 $\pm$ 0.5 Å, a value that is in reasonable agreement with the data obtained following direct incubation at pH 5.3 (see Figure 3C). Thus, both the transmembrane and peripherally bound forms of annexin B12 appear to interconvert in response to changes in pH, and both membrane forms can be converted to the soluble form of the protein at neutral pH.

Freeze-Fracture Analysis of Different pH-Dependent Membrane-Bound Forms of Annexin 12. The EPR data presented above provide structural information on a single helical hairpin region of the annexin B12 molecule. To obtain a more comprehensive overview of the Ca^{2+}-independent membrane topology of the entire protein, freeze-fracture electron microscopy experiments were performed. This method splits bilayers to produce complementary fracture faces, where integral membrane proteins appear as distinct particles but peripheral membrane proteins are not detected (*29*, *30*). Visual inspection of micrographs of freeze-fractured vesicles that had been incubated with annexin B12 at pH 4.0 revealed images of classical membrane particles (parts A and B of Figure 6). In contrast, no particles were observed in vesicles incubated with annexin B12 at pH 5.3 (Figure 6C) or in control vesicles in the absence of the protein at pH 4.0 (Figure 6D). The diameters of the transmembrane annexin B12 particles at pH 4.0 were measured as described in the Experimental Procedures. The size distribution of the

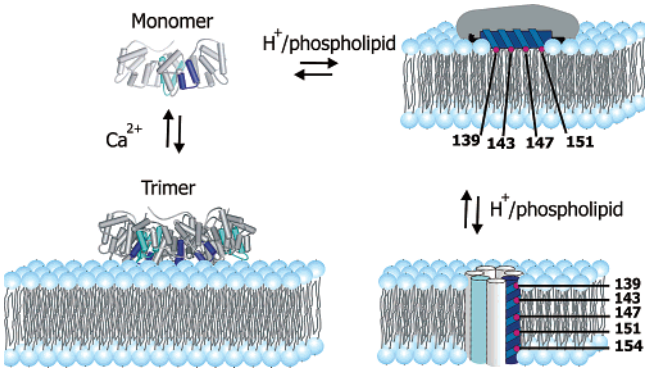

FIGURE 7: Summary of the various Ca^{2+}-dependent and Ca^{2+}-independent membrane-bound forms of annexin B12. Annexin B12 is a monomer in solution but forms a trimer following Ca^{2+}-dependent binding to the surface of bilayers. The soluble monomer and the membrane-bound trimer have backbone folds similar to the crystal structure of the protein. At mildly acidic pH, annexin B12 can undergo Ca^{2+}-independent membrane interactions that involve global refolding and conversion of helical hairpin regions (highlighted in light and dark blue) into continuous amphipathic helices with one face exposed to the hydrophobic core of the bilayer. At pH 4, the amphipathic helices are transmembrane, but near pH ~5, the helical region examined in this study was peripheral and approximately parallel to the membrane. The peripheral form identified in this study is drawn as an intermediate structure between the soluble and transmembrane structure. While the indicated transitions were observed in the present study, future experiments are required to demonstrate that the peripheral form serves as a necessary kinetic intermediate during transmembrane insertion. It should be noted that the present study only studied the conformational reorganization of one helical hairpin of the solution structure. Other regions of the peripherally bound annexin B12 are schematically indicated by gray shading. Although not directly tested in the present study, it is possible that other helical hairpins could also undergo reorganization into peripheral α helices.

particles was fairly uniform, and the majority (63%) of the particles were measured between 61 and 80 Å in diameter. These data are consistent with a model in which each molecule of transmembrane annexin B12 consists of several transmembrane helices. Very few particles were observed in the 140 Å size range. The significance of these larger particles, if any, is unknown, but the size is consistent with a dimer of the median-sized particles.

DISCUSSION

Together with previous structural analysis, the present study demonstrates that annexin B12 can exist in at least four distinctively different states: a soluble state of known crystal structure, a Ca^{2+}-dependent surface-bound trimer (*6*), a pH-dependent peripherally bound form, and a pH-dependent transmembrane form (Figure 7 and refs *12*, *13*, and *16*). The structure of the Ca^{2+}-dependent membrane-bound form is closely related to the crystal structure of the soluble protein (*5*, *6*). In contrast, Ca^{2+}-independent binding to membranes at mildly acidic pH induced major conformational reorganizations (Figures 5 and 6 and refs *12*, *13*, and *16*).

There are a number of similarities and differences between the structures of the two different pH-dependent membrane-bound forms. In both cases, the D−E helical hairpin region of repeat 2 (residues 139−155) underwent inside-out refolding that brought buried hydrophobic residues of the solution structure into contact with the hydrophobic part of the membrane (Figure 5 and ref *16*). Furthermore, in both cases, the helix−loop−helix structure was converted into a continuous amphipathic α helix (Figure 5 and ref *16*). The main difference between the two forms was that, in the pH range of ~5.0−5.5, this helical structure was peripheral and approximately parallel to the membrane surface, while at pH values below 4.5, this helical structure was transmembrane (Figures 3, 5, and 6 and ref *16*).

Freeze-fracture electron microscopic images of vesicles incubated with annexin B12 at pH 4.0 showed the presence of classic transmembrane particles (parts A and B of Figure 6), thus providing strong independent confirmation of the transmembrane formation at pH 4.0. A recent SDSL study showed that the A−B helix−loop−helix region in the fourth repeat of annexin B12 also underwent inside-out refolding and was converted into a continuous transmembrane helix at pH 4.0 (*13*). On the basis of these studies and on the analysis of the amino acid sequence in homologous repeats, we proposed that there are approximately seven helix−loop−helix regions in annexin B12 that can refold into transmembrane helices (*13*, *16*). Other studies have shown that this form of the protein is mainly monomeric (*21*). The median diameter of the freeze-fracture particles detected in membranes incubated with annexin B12 at pH 4.0 was in the 61−80 Å size range. The size of freeze-fracture particles is determined by the thickness of the metal replica and by the number of transmembrane helices in any given protein (*30*). Although we cannot determine the exact number of transmembrane helices that contribute to the freeze-fracture particles formed by annexin B12, the size of the observed particles (parts A and B of Figure 6) is consistent with our proposal that the structural form of annexin B12 having channel-like activity contains approximately seven transmembrane helices (*13*, *16*).

In contrast to the particles seen at pH 4.0, freeze-fracture images of annexin B12 containing liposomes at pH 5.3 showed no evidence of significant membrane penetration (Figure 6C). These data are consistent with EPR analysis, showing that the average immersion depth of the lipid-exposed sites in the 139−151 region was on the order of ~4−7 Å (Figure 5C). Given the fact that R1 side chains are typically ~7−10 Å away from the center of a helix (*31*, *32*), it is therefore likely that the center of the 139−151 helix is located at or slightly above the layer of the phosphates, with significant exposure to the aqueous environment. The freeze fracture data and a previous chemical-labeling study (*19*) suggest that other regions of the protein might not significantly penetrate into the phosphatidylserine containing membranes at pH 5.3 either. Considering the sequence similarity and the apparent similarity with which helical hairpins reorganize into transmembrane helices at pH 4, it is therefore possible that several other helical hairpins, aside from the region studied here, might refold into peripherally bound helices at pH 5.3.

Further studies are needed to determine whether the surface-bound form observed at intermediate pH values acts as a kinetic intermediate during the formation of the transmembrane insertion of annexin B12. The ability to convert reversibly between the different pH-bound forms strongly supports this possibility. Thus, the novel membrane-bound form of annexin B12 discovered here might provide a model system for studying the mechanism of protein-membrane insertion.

REFERENCES

1. Gerke, V., Creutz, C. E., and Moss, S. E. (2005) Annexins: Linking Ca^{2+} signalling to membrane dynamics, *Nat. Rev. Mol. Cell Biol. 6*, 449−461.
2. Moss, S. E., and Morgan, R. O. (2004) The Annexins, *Genome Biol. 5*, 219.
3. Rescher, U., and Gerke, V. (2004) Annexins−Unique membrane binding proteins with diverse functions, *J. Cell Sci. 117*, 2631−2639.
4. Seaton, B. A. (1996) *Annexins: Molecular Structure to Cellular Function* (Seaton, B. A., Ed.) R. G. Landes Company, Austin, TX.
5. Isas, J. M., Langen, R., Hubbell, W. L., and Haigler, H. T. (2004) Structure and dynamics of a helical hairpin that mediates calcium-dependent membrane binding of annexin B12, *J. Biol. Chem. 279*, 32492−32498.
6. Langen, R., Isas, J. M., Luecke, H., Haigler, T. H., and Hubbell, W. L. (1998) Membrane-mediated assembly of annexins studied by site-directed spin labeling, *J. Biol. Chem. 273*, 22453−22457.
7. Oling, F., Santos, J. S., Govorukhina, N., Mazeres-Dubut, C., Bergsma-Schutter, W., Oostergetel, G., Keegstra, W., Lambert, O., Lewit-Bentley, A., and Brisson, A. (2000) Structure of membrane-bound annexin A5 trimers: A hybrid cryo-EM−X-ray crystallography study, *J. Mol. Biol. 304*, 561−573.
8. Reviakine, I., Bergsma-Schutter, W., Mazeres-Dubut, C., Govorukhina, N., and Brisson, A. (2000) Surface topography of the p3 and p6 annexin V crystal forms determined by atomic force microscopy, *J. Struct. Biol. 131*, 234−239.
9. Luecke, H., Chang, B. T., Mailliard, W. S., Schlaepfer, D. D., and Haigler, H. T. (1995) Crystal structure of the annexin XII hexamer and implications for bilayer insertion, *Nature 378*, 512−515.
10. Swairjo, M. A., Concha, N. O., Kaetzel, M. A., Dedman, J. R., and Seaton, B. A. (1995) Ca^{2+}-Bridging mechanism and phospholipid head group recognition in the membrane-binding protein annexin V, *Nat. Struct. Biol. 2*, 968−974.
11. Golczak, M., Kicinska, A., Bandorowicz-Pikula, J., Buchet, R., Szewczyk, A., and Pikula, S. (2001) Acidic pH-induced folding of annexin VI is a prerequisite for its insertion into lipid bilayers and formation of ion channels by the protein molecules, *FASEB J. 15*, 1083−1085.
12. Isas, J. M., Patel, D. R., Jao, C., Jayasinghe, S., Cartailler, J. P., Haigler, H. T., and Langen, R. (2003) Global structural changes in annexin 12. The roles of phospholipid, Ca^{2+}, and pH, *J. Biol. Chem. 278*, 30227−30234.
13. Kim, Y. E., Isas, J. M., Haigler, H. T., and Langen, R. (2005) A helical hairpin region of soluble annexin B12 refolds and forms a continuous transmembrane helix at mildly acidic pH, *J. Biol. Chem. 280*, 32398−32404.
14. Kohler, G., Hering, U., Zschoring, O., and Arnold, K. (1997) Annexin V interaction with phosphatidylserine-containing vesicles at low and neutral pH, *Biochemistry 36*, 8189−8194.
15. Lambert, O., Cavusoglu, N., Gallay, J., Vincent, M., Rigaud, J. L., Henry, J. P., and Ayala-Sanmartin, J. (2004) Novel organization and properties of annexin 2-membrane complexes, *J. Biol. Chem. 279*, 10872−10882.
16. Langen, R., Isas, J., Hubbell, W., and Haigler, H. (1998) A transmembrane form of annexin XII detected by site-directed spin labeling, *Proc. Natl. Acad. Sci. U.S.A. 95*, 14060−14065.
17. Rosengarth, A., Wintergalen, A., Galla, H. J., Hinz, H. J., and Gerke, V. (1998) Ca^{2+}-Independent interaction of annexin I with phospholipid monolayers, *FEBS Lett. 438*, 279−284.
18. Sopkova, J., Vincent, M., Takahashi, M., Lewit-Bentley, A., and Gallay, J. (1998) Conformational flexibility of domain III of annexin V studied by fluorescence of tryptophan 187 and circular dichroism: The effect of pH, *Biochemistry 37*, 11962−11970.
19. Isas, J. M., Cartailler, J. P., Sokolov, Y., Patel, D. R., Langen, R., Luecke, H., Hall, J. E., and Haigler, H. T. (2000) Annexins V and XII insert into bilayers at mildly acidic pH and form ion channels, *Biochemistry 39*, 3015−3022.
20. Ladokhin, A. S., Isas, J. M., Haigler, H. T., and White, S. H. (2002) Determining the membrane topology of proteins: Insertion pathway of a transmembrane helix of annexin 12, *Biochemistry 41*, 13617−13626.
21. Ladokhin, A. S., and Haigler, H. T. (2005) Reversible transition between the surface trimer and membrane-inserted monomer of annexin 12, *Biochemistry 44*, 3402−3409.
22. White, S. H., Ladokhin, A. S., Jayasinghe, S., and Hristova, K. (2001) How membranes shape protein structure, *J. Biol. Chem. 276*, 32395−32398.
23. Hubbell, W. L., Gross, A., Langen, R., and Lietzow, M. A. (1998) Recent advances in site-directed spin labeling of proteins, *Curr. Opin. Struct. Biol. 8*, 649−656.
24. Columbus, L., and Hubbell, W. L. (2002) A new spin on protein dynamics, *Trends Biochem. Sci. 27*, 288−295.
25. Altenbach, C., Greenhalgh, D. A., Khorana, H. G., and Hubbell, W. L. (1994) A collision gradient method to determine the immersion depth of nitroxides in lipid bilayers: Application to spin-labeled mutants of bacteriorhodopsin, *Proc. Natl. Acad. Sci. U.S.A. 91*, 2910.
26. Reeves, J. P., and Dowben, R. M. (1969) Formation and properties of thin-walled phospholipid vesicles, *J. Cell. Physiol. 73*, 49−60.
27. Patel, D. R., Jao, C. C., Mailliard, W., Isas, J., Langen, R., and Haigler, H. (2001) Calcium-dependent binding of annexin 12 to phospholipid bilayers: Stoichiometry and implications, *Biochemistry 40*, 7054−7060.
28. Isas, J. M., Langen, R., Haigler, H. T., and Hubbell, W. L. (2002) Structure and dynamics of a helical hairpin and loop region in annexin 12: A site-directed spin labeling study, *Biochemistry 41*, 1464−1473.
29. Brandon, D. (1966) Fracture faces of frozen membranes, *Proc. Natl. Acad. Sci. U.S.A. 55*, 1048−1056.
30. Eskandari, S., Wright, E. M., Kreman, M., Starace, D. M., and Zampighi, G. A. (1998) Structural analysis of cloned plasma membrane proteins by freeze-fracture electron microscopy, *Proc. Natl. Acad. Sci. U.S.A. 95*, 11235−11240.
31. Jao, C. C., Der-Sarkissian, A., Chen, J., and Langen, R. (2004) Structure of membrane-bound α-synuclein studied by site-directed spin labeling, *Proc. Natl. Acad. Sci. U.S.A. 101*, 8331−8336.
32. Langen, R., Oh, K. J., Cascio, D., and Hubbell, W. L. (2000) Crystal structures of spin labeled T4 lysozyme mutants: Implications for the interpretation of EPR spectra in terms of structure, *Biochemistry 39*, 8396−8405.

BI052143+